Q3T Prisms: A Linear-Quadratic Solid Shell Element for Elastoplastic Surfaces

JUAN SEBASTIAN MONTES MAESTRE, ETH Zürich, Switzerland
STELIAN COROS, ETH Zürich, Switzerland
BERNHARD THOMASZEWSKI, ETH Zürich, Switzerland

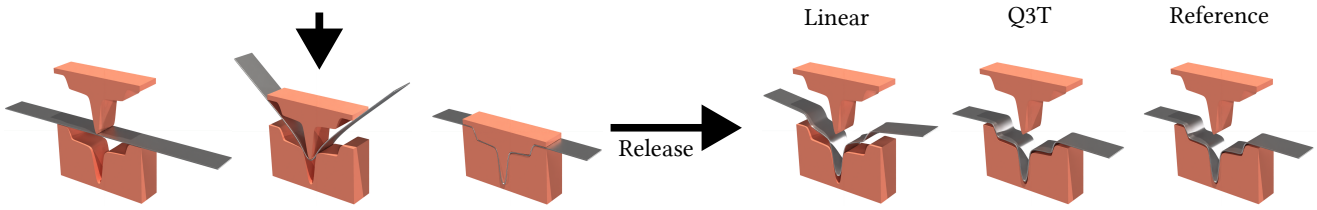

Fig. 1. Plastic forming with solid shell elements. *Left*: a metal beam is pressed into a rigid mold, experiencing bending stresses that lead to plastic deformations, and released. *Right*: quadratic-through-the-thickness (Q3T) elements closely track the reference solution, whereas linear prisms predict excessive spring-back.

We introduce an approach for simulating elastoplastic surfaces using quadratic through-the-thickness (Q3T) solid shell elements. Modeling the mechanics of deformable surfaces has been a cornerstone of graphics research for decades. Although thin shell models are suitable for many materials and applications, simulation-based planning of plastic forming processes requires attention to deformation in the thickness direction. Building on recent advances in the graphics community, we explore solid shell elements for modeling elastoplastic surfaces. Linear prism elements perform well for compressible materials such as thick cloth and foam mats. However, due to their inability to capture non-constant strain in the thickness direction, they suffer from severe locking artifacts when applied to incompressible and plastic materials. Q3T elements address this limitation with a minimal yet effective modification to linear prisms, resulting in significantly improved performance with only a moderate increase in computational cost. Through various examples, we demonstrate that Q3T elements closely match the qualitative behavior of reference simulations and provide accurate quantitative results compared to real-world deep drawing experiments.

CCS Concepts: • **Computing methodologies** → **Physical simulation**; *Shape modeling*.

Additional Key Words and Phrases: Solid Shells, Plasticity, Thickness, Incompressible Materials

ACM Reference Format:
Juan Sebastian Montes Maestre, Stelian Coros, and Bernhard Thomaszewski. 2024. Q3T Prisms: A Linear-Quadratic Solid Shell Element for Elastoplastic Surfaces. In *SIGGRAPH Asia 2024 Conference Papers (SA Conference Papers '24), December 03–06, 2024, Tokyo, Japan.* ACM, New York, NY, USA, 9 pages. https://doi.org/10.1145/3680528.3687697

Authors' Contact Information: Juan Sebastian Montes Maestre, ETH Zürich, Switzerland, juans.montes@gmail.com; Stelian Coros, ETH Zürich, Switzerland, scoros@inf.ethz.ch; Bernhard Thomaszewski, ETH Zürich, Switzerland, bthomasz@inf.ethz.ch.

SA Conference Papers '24, December 03–06, 2024, Tokyo, Japan

ACM ISBN 979-8-4007-1131-2/24/12
https://doi.org/10.1145/3680528.3687697

1 Introduction

Modeling the mechanical behavior of deformable surfaces made from fabric, rubber, or metal has been a core focus of graphics research since many decades. A two-dimensional treatment in terms of thin shell mechanics is a suitable and effective choice for many materials and applications. In this work, however, we focus on elastoplastic surfaces that require attention to deformation in the thickness direction.

Deep drawing is a prime example for elastoplastic surfaces where thin sheets of metal are shaped into desired forms. During this process, the elastoplastic sheets undergo extreme and irreversible deformations in both in-plane and thickness directions. Simulation-based planning of such plastic forming processes is highly challenging. Accurately capturing the transfer between elastic and plastic deformations is crucial to predict post-forming equilibrium shapes. Moreover, predicting deformations in the thickness direction is essential for preventing excessive thinning and rupture. Since thin shell elements are inherently unable to model these effects, volumetric finite element simulations with high-resolution meshes remain the gold standard in this context. However, the computational costs of this approach are often substantial.

An efficient alternative to generic finite element simulations is to use solid shell elements. These elements are constructed by extruding triangles or quadrilaterals along their normal direction, thus defining thin volumetric elements. Bending is captured as through-the-thickness variation of in-plane strains that induce both tensile and compressive stresses. Unlike thin shell models, solid shell elements capture deformation through-the-thickness, and they integrate seamlessly with well-established 3D elastoplastic constitutive laws. Recent work from the graphics community has shown that linear prism elements are an efficient choice for design and animation of thick sheet materials [Chen et al. 2023; Montes et al. 2023]. Unfortunately, when applied to incompressible materials and plastic

deformations, linear prisms exhibit severe locking artefacts, making them virtually unusable in this context.

In this work, we propose a minimal modification of linear prisms that resolves locking artifacts. As shown in previous work [Hauptmann and Schweizerhof 1998; Sansour 1995], the poor performance of linear prisms is due to their inability to capture non-constant strain in the thickness direction. This observation motivates replacing the linear displacement interpolation in the thickness direction with a quadratic one while keeping the in-plane approximation unchanged [Harnau and Schweizerhof 2002]. We follow this strategy and add displacement degrees of freedom to the mid-surface of a linear prism element to obtain a quadratic through-the-thickness (Q3T) element. As we show through a range of examples, Q3T elements enjoy vastly improved performance with only moderate increase in computation cost. Unlike linear prisms, Q3T elements faithfully track the qualitative behavior of reference solutions for large deformations of incompressible and plastic sheet materials. We furthermore demonstrate that these elements offer good quantitative accuracy in comparison to real-world deep drawing experiments.

2 Related Work

Thin Shells in Graphics. Modeling elastic surfaces has been a core focus of graphics for almost four decades [Terzopoulos et al. 1987]. Arguably the most widely used class of bending models are based on discretizations of the shape operator [Bridson et al. 2003; Gingold et al. 2004; Grinspun et al. 2003, 2006]. Cubic shells [Garg et al. 2007] simplify nonlinear bending models to a low-degree polynomial that can be evaluated efficiently, albeit at reduced accuracy. Quadratic approximations [Bergou et al. 2006; Volino and Magnenat-Thalmann 2006] simplify even more but offer constant Hessian with guaranteed positive-definiteness, helping both stability and speed.

Instead of using piece-wise linear discretizations, another line of work has investigated the use of higher-order finite-elements for thin shell mechanics [Cirak and Ortiz 2001; Cirak et al. 2000; Guo et al. 2018; Le et al. 2023; Thomaszewski et al. 2006].

Beyond purely elastic bending, extensions of shell models towards various effects have been explored including viscosity [Batty and Bridson 2008], plasticity [Chen et al. 2018], sound [Chadwick and James 2011], magnetic effects [Chen et al. 2022], interaction with sharp objects [Weidner et al. 2018], and coupling with rods [Pérez et al. 2017]. Another line of research has investigated refinement methods such as to mitigate the impact of discretization on simulations with smooth folds [Narain et al. 2012], sharp creases [Narain et al. 2013a], wrinkling [Chen et al. 2021; Rémillard and Kry 2013], fracture patterns [Pfaff et al. 2014] and multi-layer thin plates [Busaryev et al. 2013]. Extensive research has also been devoted to the accurate modeling of thin shell material properties [Miguel et al. 2012; Wang et al. 2011; Wen and Barbič 2023].

While these existing models for deformable surfaces cover a large range of effects and phenomena, none of them account for through-the-thickness deformations, which is the focus of our work.

Plasticity. Modeling elastoplastic materials has a comparatively long history in graphics [O'Brien 2002; Terzopoulos and Fleischer 1988]. As a conceptual connection to incompressibility, the plastic deformations observed in real-world materials are often purely deviatoric, i.e., volume-preserving. Plasticity often goes along with large distortions that mandate mesh adaptation strategies to maintain well-shaped elements [Bargteil et al. 2007; Ferguson et al. 2023; Wicke et al. 2010; Wojtan et al. 2009]. Avoiding re-meshing altogether, point-based methods [Gerszewski et al. 2009; Jones et al. 2014; Müller et al. 2004], including variants based on SPH [Gissler et al. 2020] and MPM [Fang et al. 2019; Klár et al. 2016], are an attractive alternative for simulating large elastoplastic deformations. While the above methods target volumetric materials, few works explicitly consider elastoplastic surfaces. A notable exception is the work by Narain et al. [2013b] and Chen et al. [2018]. However, their surface-based formulations cannot account for deformation in the thickness direction, which is the focus of our work.

Solid Shells. Solid shells have been introduced in the mechanics community as an alternative to surface-based thin shell elements [Parisch 1995]. Instead of a mid-surface patch, solid shell elements represent a volumetric region that can extend through the entire thickness of the shell. While this requires more nodes in general, solid shell elements avoid non-kinematic variables (rotations, tangents) and reduce requirements on continuity across elements [Hauptmann and Schweizerhof 1998]. There are many options for constructing solid shell elements, including the widely used triangular and quadrilateral prisms with linear and quadratic interpolation functions [Hauptmann et al. 2000]. Solid shells can serve as a replacement for thin shell elements, but they are most attractive for applications that involve through-the-thickness deformations and stresses [Hauptmann et al. 2001]. Recent work by Montes et al. [2023] and Chen et al. [2023] from the graphics community has shown the potential of low-order solid shell elements for compressible materials such as cloth and foam. For incompressible materials and plastic deformations, however, linear prism elements show severe *locking* artefacts that render them virtually unusable for applications [Doll et al. 2000].

Locking. Locking is a phenomenon that manifests as finite element solutions converging very slowly under refinement. For shells, locking can be categorized into shear locking and Poisson locking [Babuška and Suri 1992; Zienkiewicz et al. 2013]. Shear locking refers to the inability of low-order elements to model pure states of bending, which introduces parasitic shear strain. Poisson locking occurs for elements with low-order through-the-thickness interpolation and is especially severe for thin, quasi-incompressible materials. A plethora of strategies aiming to alleviate locking have been presented, including reduced integration [Arnold and Brezzi 1997], enhanced assumed strain (EAS) [Simo and Rifai 1990], and assumed natural strain (ANS) [Hughes and Tezduyar 1981]. Locking has likewise been investigated in graphics. For example, Irving et al. [2007] use nodal averaging when evaluating pressure constraints to avoid Poisson locking for incompressible solids. With a similar goal in mind, Francu et al. [2021] obtain locking-free tetrahedra by augmenting nodes with an additional degree of freedom. English and Bridson [2008] resorted to Crouzeix-Raviart elements such as to avoid shear locking in cloth simulation.

We experimentally assess the practical impact of locking in solid shell elements when applied to incompressible materials and volume-preserving plastic deformations. Previous work has shown that the main source of locking observed in low-order solid shell elements is their linear interpolation in the thickness direction [Hauptmann and Schweizerhof 1998]. Solutions to this problem have been proposed based on EAS and ANS methods or by increasing the interpolation order in the thickness direction with additional variables [Harnau and Schweizerhof 2002; Sansour 1995]. We follow the second strategy and demonstrate its effectiveness for triangular prism solid shell elements. By replacing the linear interpolation in the thickness direction with a quadratic one, Q3T elements prevent locking artefacts while avoiding the steep increase in cost and complexity associated with fully quadratic or higher-order elements.

3 Method

We start by describing our approach for generating and simulating elastoplastic solid shells. We then review linear prism elements and analyze their limitations for incompressible and plastic materials. We show that linear prismatic elements suffer from the same limitations as linear quadrilateral solid shells [Hauptmann et al. 2001]. These observations motivate our quadratic through-the-thickness prismatic element (Q3T), which we introduce subsequently.

3.1 Elastoplastic Solid Shells

We generate solid shells with prismatic elements given a triangle mesh as input. This input triangle mesh determines the mid-surface of the solid shell and we denote its vertices as $\mathbf{x}^m$. We create two offset surfaces by extruding mid-surface nodes along their corresponding vertex normal. The vertices of the resulting top and bottom surfaces are denoted as $\mathbf{x}^t$ and $\mathbf{x}^b$, respectively. From these triangle meshes, we define a prismatic solid shell element for each face of the input mesh. For each such element, we interpolate nodal positions to obtain a continuous geometry field as

$$\mathbf{x}(u,v,w) = \sum_i N_i(u,v,w)\mathbf{x}_i \,, \tag{1}$$

where $N_i : (u,v,w) \to \mathbb{R}$ are piece-wise polynomial basis functions. The parametric coordinates u, v and w correspond to in-plane and thickness directions, respectively. With this generic interpolation scheme, the deformation gradient follows in the usual way as

$$\mathbf{F}(u,v,w) = \frac{\partial \mathbf{x}}{\partial \mathbf{X}} = \sum_i \nabla N_i \mathbf{x}_i^T \,. \tag{2}$$

The stored elastic energy of a deformed solid shell is obtained by integrating the elastic energy density $\Psi(\mathbf{F})$ across its domain Ω,

$$W_{\text{el}} = \int_\Omega \Psi(\mathbf{F}(u,v,w))\, dV = \sum_e \int_{\Omega_e} \Psi(\mathbf{F}(u,v,w))\, dV \,, \tag{3}$$

where Ω_e denote per-element parameteric domains. Evaluating the corresponding per-element integrals requires numerical quadrature, which amounts to a weighted sum of energy densities evaluated at a set of quadrature points $\mathbf{p}_i = (u_i, v_i, w_i)$ with corresponding weights α_i.

Simulation. Static and dynamic equilibrium configurations of elastoplastic solid shells are computed by minimizing a generalized potential including elasticity, plasticity, and inertia terms. For dynamic problems, we use the optimization-based formulation of implicit Euler [Martin et al. 2011].

For plastic materials, the deformation gradient is decomposed into elastic and plastic components as $\mathbf{F} = \mathbf{F}_{\text{el}}\mathbf{F}_{\text{pl}}$. Plastic deformation gradients are stored at quadrature points and updated according to plastic flow rules. We follow Li et al. [2022] to likewise incorporate plasticity in variational form. Please see the supplemental material for details.

3.2 Linear Prism Elements

Linear prism elements are constructed from two corresponding triangle elements from the top and bottom surface of the solid shell, see Fig. 2, *left*. The shape functions take the form

$$N_1(u,v) = u, \quad N_2(u,v) = v, \quad N_3(u,v) = 1 - u - v \,, \tag{4}$$

and the corresponding interpolation is

$$\mathbf{x}(u,v) = \sum_i N_i(u,v)\mathbf{x}_i \,, \tag{5}$$

where $0 \le u \le 1$ and $0 \le v \le 1 - u$. We then interpolate linearly through the thickness to obtain a linear geometry field as

$$\mathbf{x}(u,v,w) = \frac{1}{2}(w-1)\mathbf{x}_b(u,v) + \frac{1}{2}(w+1)\mathbf{x}_t(u,v) \,, \tag{6}$$

with $-1 \le w \le 1$. Linear prisms have a total of 6 nodes with 18 DoFs.

Analysis. As demonstrated by Montes et al. [2023] and Chen et al. [2023], linear prism elements can produce acceptable accuracy for compressible sheet materials such as thick cloth and foam mats. With increasing Poisson ratio, however, linear prisms show an extremely stiff bending response, rendering them virtually useless even for qualitative purposes. As we show in Sec. 4, this spurious stiffening effect manifests across numerous situations: linear prisms fail to predict wrinkling for in-plane tension (Fig. 4), they produce far too little deflection under self weight (Fig. 5), and they lead to excessive spring-back in plastic forming (Figs. 1, 6, 13). We note that this effect occurs independently of the quadrature rule. In particular, the selective reduced integration rule advocated by Chen et al. [2023] does not resolve these problems.

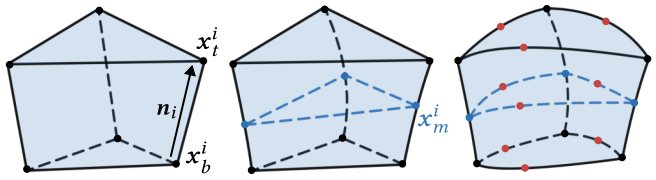

Fig. 2. Illustration of linear, quadratic through-the-thickness (Q3T), and fully quadratic prism elements (from *left* to *right*). Linear prisms have only 6 nodes and two integration points, Q3T elements have 9 nodes and 3 integration points, whereas fully quadratic prisms have 18 nodes and 21 integration points.

All of the above failure cases can be attributed to the inability of linear prisms to model variations in strain in the thickness direction [Hauptmann et al. 2001]. To see this, consider a simple example in which a square metal sheet is bent into a state of constant uniaxial curvature (Fig. 3). At the top surface, the in-plane deformation ε_{xx} induced through bending is *tensile* (positive) whereas it is *compressive* (negative) at the bottom surface. Depending on the material's Poisson ratio, these axial strains will generate compensating in-plane strains ε_{yy} and thickness strains ε_{zz}. Both strains must have opposite sign to the imposed axial strain, i.e., compressive at the top and tensile at the bottom surface. While linear prisms can model in-plane strain ε_{yy} that varies through the thickness, they cannot produce varying thickness strain ε_{zz} since the geometry interpolation is linear in the thickness direction. Consequently, all strain compensation must come from the in-plane component ε_{yy}, leading to a much stiffer response.

These observations explain why elements with constant strain through-the-thickness perform poorly for nearly incompressible elasticity and plasticity—and they motivate a modified version as explained next.

3.3 Q3T Prism Elements

Previous analysis has shown that the inability of linear prisms to produce non-constant strain in the thickness direction is the main source of inaccuracy [Harnau and Schweizerhof 2002; Hauptmann et al. 2001; Sansour 1995]. A natural option for improving accuracy is thus to increase the degree of interpolation through the thickness [Hauptmann et al. 2001]. As can be seen from the construction of linear prism elements, solid shell elements allow for separate in-plane and through-the-thickness interpolation schemes. We leverage this freedom to define a triangular prismatic element that uses linear in-plane but quadratic through-the-thickness interpolation. To this end, we augment the linear prism with three additional nodes $\mathbf{x}_m$ at the mid-surface (i.e., at $w = 0$). The corresponding through-the-thickness interpolation follows as

$$\mathbf{x}(u,v,w) = \frac{1}{2}w(w-1)\mathbf{x}_b(u,v)+(1-w)^2\mathbf{x}_m(u,v)+\frac{1}{2}w(w+1)\mathbf{x}_t(u,v)\,.$$

The resulting *quadratic through-the-thickness* element, or Q3T for short, is defined by 9 nodes with a total of 27 degrees of freedom. As we show in the following section, the linearly varying thickness strain of Q3T elements leads to vastly improved accuracy with only a moderate increase in computational cost.

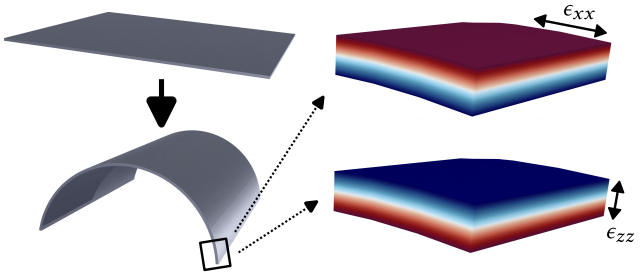

Fig. 3. Distribution of strain through the thickness as a result of cylindrical bending for materials with high Poisson's ratios.

4 Results

We perform an extensive analysis of our Q3T solid shell element and compare its performance to linear prisms. In the first part, we analyze both qualitative and quantitative performance on a set of simple experiments. In the second part, we present more complex examples that are representative of real-world use cases.

Reference Solutions. Even simple experiments involving plastic deformations generally have no closed-form solution. We therefore compare to reference solutions obtained using high-resolution simulations with fully quadratic prism elements (see Fig. 2, *right*). We selected quadratic prisms since they converged to the same solution as (even) higher-order elements in our experiments. See also Fig. 8.

4.1 Basic Analysis

In-plane Stretching. In our first experiment, we evaluate the performance of linear prisms and Q3T elements for pure stretching deformation. To this end, we clamp a square plate (70cm×70cm×0.7cm) at one edge and subject it to a uniform in-plane load perpendicular to the clamped edge. To assess potential locking artefacts, we perform the test with different Poisson ratios. As can be seen in Fig. 4, all elements perform well for $\nu = 0$, which leads to simple uniaxial stretching without any normal displacement. For $\nu = 0.3$, all elements properly capture the lateral displacements of the plate as a result of the Poisson's ratio. However, as the material approaches the incompressible limit, only Q3T prisms are able to capture the low-frequency buckling deformations seen in the reference solution, whereas linear prisms lead to a planar state with much larger in-plane stresses. We note that the solution obtained with linear prisms is at a stable equilibrium point as the Hessian is positive definite. We conjecture that, due their inability to capture pure states of bending, out-of-plane buckling would lead to even higher stresses for the linear prisms.

Cantilever Beam. In our second benchmark, we test the performance of linear prisms and Q3T elements under pure bending loads. To this end, we consider a rectangular cantilever beam (70cm × 7cm × 0.7cm) clamped at one end and subjected to a uniform load in the normal direction. We compare results for different mesh resolutions to the reference solution. As can be seen in Fig. 5, both elements perform qualitatively well for low Poisson's ratios. For high Poisson's ratios, however, linear prisms become extremely stiff, rendering them unusable even for qualitative purposes. By contrast, Q3T elements are much more accurate and produce deflections close to the reference solution. The remarkable accuracy of Q3T elements in this test is explained by their ability to represent linear strain variations in the thickness direction (Fig. 3), which are vital for pure bending deformations.

Plastic Bending. Plastic deformations are driven by the deviatoric strain tensor, which can be expressed as $\mathbf{H}_{\text{dev}} = \mathbf{H} - \frac{1}{3}\text{tr}(\mathbf{H})$, where $\mathbf{H}$ is the Hencky strain tensor (see supplemental material). Similar to the cantilever beam example, linear prisms tend to overestimate the trace of the strain tensor for high Poisson's ratio since they can only

model constant strain in the thickness direction. This, in turn, leads to an underestimation of the deviatoric strain and, consequently, plastic deformation.

We test this hypothesis by cylindrically bending an elastoplastic beam with a steel-like material beyond its elastic regime. We use a Young's modulus of $E = 200$ GPa, a Poisson's ratio of $\nu = 0.33$, and a yield stress of $\sigma_y = 16$ MPa. After the deforming force is removed, we study the residual deformation. As can be seen from Fig. 6, linear prisms do not retain as much plastic deformation as the reference solution. By contrast, Q3T elements predict residual stresses similar to the reference solution, with only minor deviations due to parasitic shear stress.

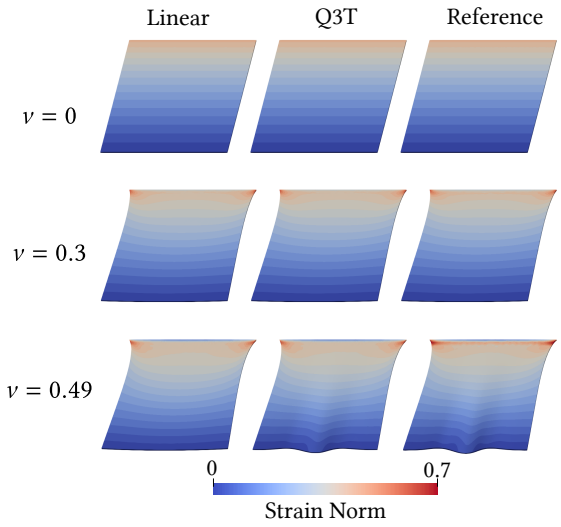

Fig. 4. Comparison of solid shell elements on a square plate (70cm × 70cm × 0.7cm) that is stretched using uniform in-plane loading. Both element types properly capture stretching for moderate Poisson ratios (top and middle row). For almost incompressible materials (bottom row), only Q3T elements correctly capture the out-of-plane buckling observed in the reference solution.

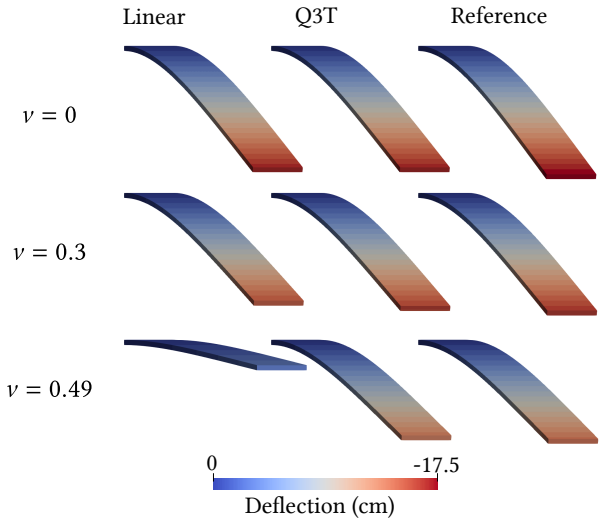

Fig. 5. Deflections of a uniformly-loaded cantilever plate for linear prisms and Q3T elements using different Poisson ratios. Linear prisms struggle increasingly as Poisson's ratio approaches the incompressible limit.

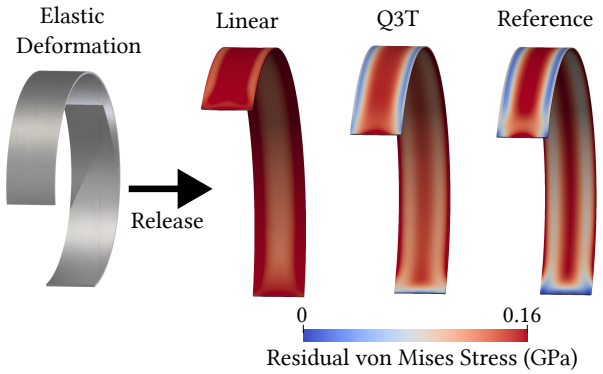

Fig. 6. Plastic deformation of a bent beam after release. Linear prisms underestimate plastic deformations compared to the reference solution. The residual stress obtained with our Q3T elements is close to the reference solution.

Performance. To assess the computational performance of Q3T elements, we compare timings for factorizing the Hessian of the elastic energy for the cantilever beam example show in Fig. 5. As can be seen from the plot shown in Fig. 7 (*left*), linear prisms are roughly twice as fast for the same number of elements. Nevertheless, Q3T elements are several times faster than fully quadratic prisms. When comparing computation times for the same number of degrees of freedom (Fig. 7, *right*), Q3T elements are roughly 40% slower than linear prisms, but 30% faster than quadratic prisms. To put these timings in perspective, it should be emphasized that Q3T elements tend to produce the same qualitative behavior as fully quadratic prisms (for equal numbers of nodes), whereas linear prisms exhibit

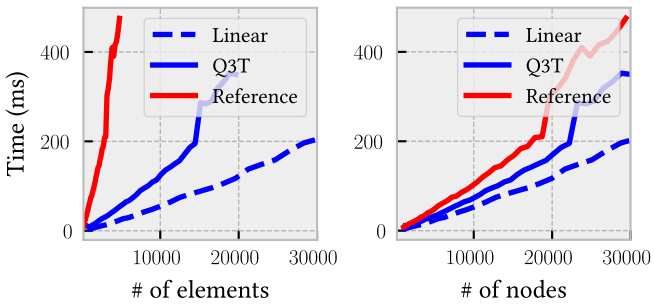

Fig. 7. Cholesky decomposition of the Hessian of linear and Q3T elements compared to the reference solution for the cantilever beam example using the same number of elements (*left*) and same number of nodes (*right*).

severe locking artefacts. See also Table 1 for timings and statistics for all examples presented in this section.

Convergence under Refinement. Linear elements are known to lock for materials with high Poisson's ratios and pure bending deformations. To assess this behavior in Q3T elements, we study their convergence under refinement against linear and fully quadratic elements on a clamped cantilever subjected to uniform loading. We use a single layer of elements and a Poisson's ratio of $\nu = 0.499$. As can be seen in Fig. 8, fully linear elements fail to converge to the reference solution due to Poisson locking. In contrast, Q3T elements reach an acceptable solution for a sufficiently dense discretization, although convergence is slower compared to higher-order elements.

4.2 Applications

In the following paragraphs, we present a series of examples that highlight different use cases of elastoplastic surfaces modeled with solid shell elements.

Plastic Forming. To demonstrate the importance of accurate plastic deformations on a practical use case, we simulate a sheet metal forming process. As shown in Fig. 1, linear elements are unable to accurately capture plastic deformations, leading to significant spring-back after release. By contrast, Q3T elements closely match the post-release state predicted by the reference solution[1].

As a second use case, we study the performance of solid shell elements in simulating the manufacturing process for a custom cookie cutter. The cookie cutter is made from a circular aluminum strip that is punched into a die with the desired shape. As can be seen in Fig. 13, linear prisms shear excessively towards the boundaries of the strip such as to release volumetric stress. Q3T elements, in contrast, properly capture the plastic deformations and thus avoid excessive shearing and spring-back.

Deep Drawing. We furthermore test the ability of Q3T elements to capture very large plastic deformations by simulating the deep drawing process of a plastic cup. To validate our simulations, we replicate the setup from Coër et al. [2018], consisting of a punch, a blank holder, and a die as shown in Fig. 9. For details on the setup please refer to the original paper. To simulate contact, we model the punch, blank holder, and die using smooth signed distance functions[2]. For every vertex of the blank mesh, we evaluate the distance functions and penalize negative values. During the deep-drawing process, radial cross-sections of the blank must slide through the radius of the die as it deforms. To accurately capture this behavior, we follow a strategy similar to Coër et al. [2018] and discretize the blank such that the distance between neigboring vertices is less than 0.5mm. The punch performs a vertical translation through the die, deforming a 1mm thick metal blank, which is furthermore constrained by the walls of the die. The blank holder presses the boundary of the blank against the die. Without the blank holder, the cup would wrinkle at the boundary, see Fig. 12.

The deep-drawing process can be structured into three stages (see Fig. 10). First, the blank is shaped to conform to the rim of the die. During this stage, the blank experiences a slight thinning at the rim due to bending. After the top surface of the cup has been formed, the bowl of the cup is shaped. In this second stage, the blank is subjected to compressive stresses that lead to thickening as it is pushed through the die. In the final thinning stage, the thickened blank must pass through the gap between the punch and the die, which reduces its thickness to the gap size.

During the entire process, the volume of the blank must be preserved. Due to the inability of linear prisms to model non-constant strain in the thickness direction, simulation with this element leads to failure (Fig. 11). Q3T elements are not only able to properly capture the deformation of the cup, but also produce forces with similar accuracy as the reference solution in comparison to experimental data (Fig. 14).

[1] Using again a high-resolution simulation with fully quadratic elements.

[2] See also https://iquilezles.org/articles/distfunctions/

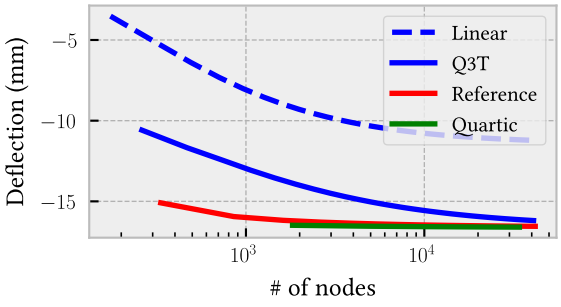

Fig. 8. Convergence under refinement for a cantilever beam simulated with one layer of elements. The linear-log plot shows comparisons between linear prisms, Q3T elements, quadratic prisms (reference), and quartic prisms.

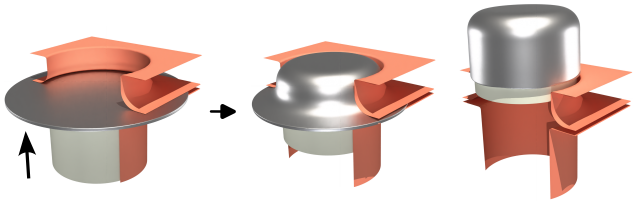

Fig. 9. Deep drawing of a plastic cup. The setup consists of a metal blank, a punch (*yellow*), a die (*red-top*) and a blank holder (*red-bottom*).

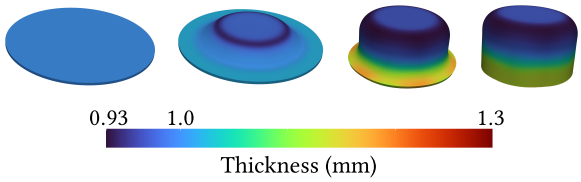

Fig. 10. Thickness variations of the plastic cup during the forming process. From left to right: undeformed blank, thinning on the rim of the cup, thickening due to compression, and final cup after thinning.

Table 1. Summary of statistics for all our experiments.

Example	# Nodes	# Elements	Avg. time/iter [s]	Figure
Cup (Linear)	27100	26718	0.812	Fig. 12-*left*
Cup (Q3T)	40650	26718	1.887	Fig. 12-*center*
Cup (Reference)	41800	6870	2.525	Fig. 12-*right*
Beam (Linear)	4814	4504	0.184	Fig. 1-*left*
Beam (Q3T)	7221	4504	0.298	Fig. 1-*center*
Beam (Reference)	7221	1126	0.372	Fig. 1-*right*
Cookie Cutter (Linear)	5762	5311	0.186	Fig. 13-*b-left*
Cookie Cutter (Q3T)	8643	5311	0.306	Fig. 13-*b-right*

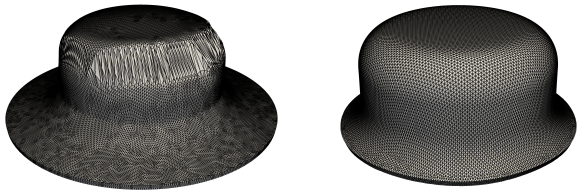

Fig. 11. *Left*: Simulating the plastic cup with linear elements results in failure. Due to their inability to model linear strains through the thickness, they shear instead. *Right*: Q3T elements properly capture the deformation of the cup.

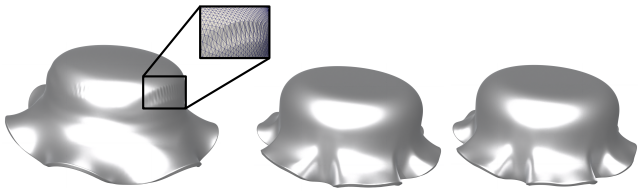

Fig. 12. Simulation of the plastic cup without the support of the blank holder. Under these conditions, the cup wrinkles due to the compressive forces exerted by the die. Q3T (*center*) elements produce similar wrinkling patterns as the reference solution (*right*), whereas linear prisms (*left*) produce qualitatively different results with excessive shearing (inset).

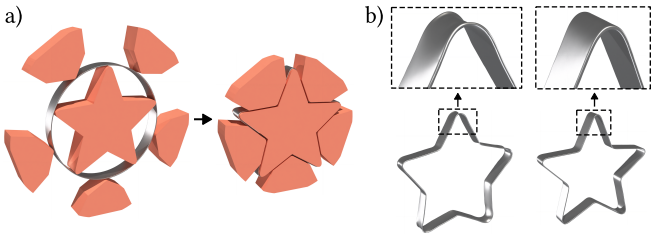

Fig. 13. Plastic forming of a star-shaped cookie cutter. *a*) A circular aluminum strip is pressed into a star-shaped die by 5 punches. *b*) The resulting strip after deformation using linear (*left*) and Q3T (*right*) elements. linear elements produce excessive shearing towards the boundaries of the strip, while Q3T elements properly capture plastic bending deformation.

5 Conclusions

We explored a solid shells with triangular prisms elements for efficient modeling of elastoplastic surfaces. We see the primary appeal of Q3T elements for applications where a triangle mesh of sufficiently high resolution is provided as input and coarsening is undesirable. While fully quadratic and quartic solid shell elements would obviously provide more accurate solutions, our Q3T elements will be substantially faster while avoiding the unacceptable artefacts of linear prisms.

5.1 Limitations and Future Work

For the same number of nodes, Q3T elements significantly reduce locking compared to linear prisms. They also lead to much less overhead than fully quadratic elements and are therefore an attractive option for both animation and simulation-based planning. However, convergence under refinement is slower than for fully quadratic elements. If ultimate accuracy is the top priority, fully quadratic elements are likely preferable.

Our simple examples already indicate that deep drawing is a highly complex process where small variations in parameters can lead to large changes in the resulting product. While we have only considered forward simulation in this work, using Q3T elements for inverse design of elastoplastic forming is an exciting direction for future work.

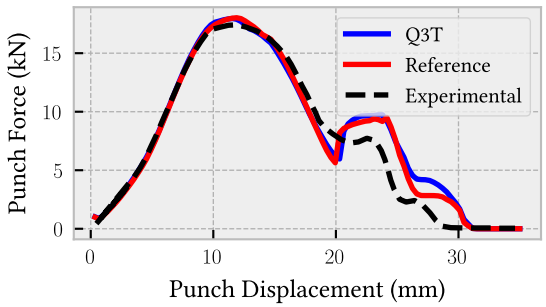

Fig. 14. Forces measured at the punch for the simulation of the plastic cup. Q3T elements produce a similar force output to the reference solution and real-world experiments [Coër et al. 2018].

Solid shell elements directly support 3D constitutive models, which simplifies the simulation of phenomena such as plasticity and growth, but also fracture and crack propagation. These capabilities seem an ideal basis for modeling (and optimizing) the complex fabrication process of ceramic shells [Hergel et al. 2019], including extrusion-based manufacturing, moisture transport and drying, as well as firing.

Acknowledgments

We are grateful to the anonymous reviewers for their valuable comments. This work was supported by the European Research Council (ERC) under the European Union's Horizon 2020 research and innovation program (grant agreement No. 866480), and the Swiss National Science Foundation through SNF project grant 200021_200644.

References

Douglas N. Arnold and Franco Brezzi. 1997. Locking-free finite element methods for shells. *Math. Comp.* 66 (1 1997), 1–15. Issue 217. https://doi.org/10.1090/S0025-5718-97-00785-0

Ivo Babuška and Manil Suri. 1992. Locking effects in the finite element approximation of elasticity problems. *Numer. Math.* 62 (12 1992), 439–463. Issue 1. https://doi.org/10.1007/BF01396238

Adam W. Bargteil, Chris Wojtan, Jessica K. Hodgins, and Greg Turk. 2007. A finite element method for animating large viscoplastic flow. In *ACM SIGGRAPH 2007 Papers* (San Diego, California) *(SIGGRAPH '07)*. Association for Computing Machinery, New York, NY, USA, 16–es. https://doi.org/10.1145/1275808.1276397

Christopher Batty and Robert Bridson. 2008. Accurate Viscous Free Surfaces for Buckling, Coiling, and Rotating Liquids. In *Eurographics/SIGGRAPH Symposium on Computer Animation*, Markus Gross and Doug James (Eds.). The Eurographics Association. https://doi.org/10.2312/SCA/SCA08/219-228

Miklos Bergou, Max Wardetzky, David Harmon, Denis Zorin, and Eitan Grinspun. 2006. A Quadratic Bending Model for Inextensible Surfaces. In *Proceedings of the Fourth Eurographics Symposium on Geometry Processing* (Cagliari, Sardinia, Italy) *(SGP '06)*. Eurographics Association, Goslar, DEU, 227–230.

Robert Bridson, Sebastian Marino, and Ronald Fedkiw. 2003. Simulation of clothing with folds and wrinkles. In *ACM SIGGRAPH/Eurographics Symposium on Computer Animation (SCA) 2003*.

Oleksiy Busaryev, Tamal K. Dey, and Huamin Wang. 2013. Adaptive Fracture Simulation of Multi-Layered Thin Plates. *ACM Trans. Graph.* 32, 4, Article 52 (jul 2013), 6 pages. https://doi.org/10.1145/2461912.2461920

Jeffrey N. Chadwick and Doug L. James. 2011. Animating Fire with Sound. *ACM Transactions on Graphics (Proceedings of SIGGRAPH 2011)* 30, 4 (Aug. 2011). http://www.cs.cornell.edu/projects/Sound/fire

Hsiao Yu Chen, Arnav Sastry, Wim M. Van Rees, and Etienne Vouga. 2018. Physical simulation of environmentally induced thin shell deformation. *ACM Transactions on Graphics (TOG)* 37 (7 2018), 13. Issue 4. https://doi.org/10.1145/3197517.3201395

Xuwen Chen, Xingyu Ni, Bo Zhu, Bin Wang, and Baoquan Chen. 2022. Simulation and Optimization of Magnetoelastic Thin Shells. *ACM Trans. Graph.* 41, 4, Article 61 (jul 2022), 18 pages. https://doi.org/10.1145/3528223.3530142

Yunuo Chen, Tianyi Xie, Cem Yuksel, Danny Kaufman, Yin Yang, Chenfanfu Jiang, and Minchen Li. 2023. Multi-Layer Thick Shells. In *SIGGRAPH 2023 Conference Papers (to appear)*. Association for Computing Machinery, New York, NY, USA.

Zhen Chen, Hsiao yu Chen, Danny M Kaufman, Adobe Research, H y Chen, E Vouga, D M Kaufman, Hsiao-Yu Chen, and Mélina Skouras. 2021. Fine Wrinkling on Coarsely Meshed Thin Shells. *ACM Transactions on Graphics (TOG)* 40 (8 2021). Issue 5. https://doi.org/10.1145/3462758

Fehmi Cirak and Michael Ortiz. 2001. Fully C1-conforming subdivision elements for finite deformation thin-shell analysis. *Internat. J. Numer. Methods Engrg.* 51 (7 2001), 813–833. Issue 7. https://doi.org/10.1002/NME.182

Fehmi Cirak, Michael Ortiz, and Peter Schrr Oder. 2000. Subdivision surfaces: a new paradigm for thin-shell finite-element analysis. *International Journal for Numerical Methods in Engineering Int. J. Numer. Meth. Engng* 47 (2000), 2039–2072. https://doi.org/10.1002/(SICI)1097-0207(20000430)47:12

J. Coër, H. Laurent, M. C. Oliveira, P.-Y. Manach, and L. F. Menezes. 2018. Detailed experimental and numerical analysis of a cylindrical cup deep drawing: Pros and cons of using solid-shell elements. *International Journal of Material Forming* 11, 3 (May 2018), 357–373. https://doi.org/10.1007/s12289-017-1357-4

Stefan Doll, Karl Schweizerhof, Ralf Hauptmann, and Christof Freischläger. 2000. On volumetric locking of low-order solid and solid-shell elements for finite elastoviscoplastic deformations and selective reduced integration. *Engineering Computations* 17, 7 (2000), 874–902.

Elliot English and Robert Bridson. 2008. Animating Developable Surfaces Using Nonconforming Elements. *ACM Trans. Graph.* 27, 3 (aug 2008), 1–5. https://doi.org/10.1145/1360612.1360665

Yu Fang, Minchen Li, Ming Gao, and Chenfanfu Jiang. 2019. Silly rubber: an implicit material point method for simulating non-equilibrated viscoelastic and elastoplastic solids. *ACM Trans. Graph.* 38, 4, Article 118 (jul 2019), 13 pages. https://doi.org/10.1145/3306346.3322968

Zachary Ferguson, Teseo Schneider, Danny Kaufman, and Daniele Panozzo. 2023. Intersection-Aware Timestep Remeshing for Contacting Elastodynamics. *ACM Trans. Graph.* 42, 4, Article 145 (jul 2023), 15 pages. https://doi.org/10.1145/3592428

Mihai Frâncu, Arni Asgeirsson, Kenny Erleben, and Mads J.L. Rønnow. 2021. Locking-Proof Tetrahedra. *ACM Transactions on Graphics (TOG)* 40 (4 2021). Issue 2. https://doi.org/10.1145/3444949

Akash Garg, Eitan Grinspun, Max Wardetzky, and Denis Zorin. 2007. Cubic Shells. (2007). https://doi.org/10.5555/1272690

Dan Gerszewski, Haimasree Bhattacharya, and Adam W. Bargteil. 2009. A point-based method for animating elastoplastic solids. In *Proceedings of the 2009 ACM SIGGRAPH/Eurographics Symposium on Computer Animation* (New Orleans, Louisiana) *(SCA '09)*. Association for Computing Machinery, New York, NY, USA, 133–138. https://doi.org/10.1145/1599470.1599488

Yotam Gingold, Adrian Secord, Jefferson Han, Eitan Grinspun, and Denis Zorin. 2004. A discrete model for inelastic deformation of thin shells. In *ACM SIGGRAPH/Eurographics Symposium on Computer Animation (SCA) 2004*.

Christoph Gissler, Andreas Henne, Stefan Band, Andreas Peer, and Matthias Teschner. 2020. An implicit compressible SPH solver for snow simulation. *ACM Trans. Graph.* 39, 4, Article 36 (aug 2020), 16 pages. https://doi.org/10.1145/3386569.3392431

Eitan Grinspun, Anil N Hirani Caltech, Mathieu Desbrun, and Peter Schröder Caltech. 2003. Discrete Shells. (2003). https://doi.org/10.5555/846276.846284

Eitan Grinspun, Yotam Gingold, Jason Reisman, and Denis Zorin. 2006. Computing discrete shape operators on general meshes. *Computer Graphics Forum* 25 (2006), 547–556. Issue 3. https://doi.org/10.1111/J.1467-8659.2006.00974.X

Qi Guo, Xuchen Han, Chuyuan Fu, Theodore Gast, Rasmus Tamstorf, and Joseph Teran. 2018. A material point method for thin shells with frictional contact. *ACM Transactions on Graphics* 37 (2018). Issue 4. https://doi.org/10.1145/3197517.3201346

Matthias Harnau and Karl Schweizerhof. 2002. About linear and quadratic "Solid-Shell" elements at large deformations. *Computers & Structures* 80, 9 (2002), 805–817. https://doi.org/10.1016/S0045-7949(02)00048-2

R. Hauptmann, S. Doll, M. Harnau, and K. Schweizerhof. 2001. 'Solid-shell' elements with linear and quadratic shape functions at large deformations with nearly incompressible materials. *Computers & Structures* 79, 18 (2001), 1671–1685. https://doi.org/10.1016/S0045-7949(01)00103-1

R. Hauptmann and K. Schweizerhof. 1998. A systematic development of 'solid-shell' element formulations for linear and non-linear analyses employing only displacement degrees of freedom. *Internat. J. Numer. Methods Engrg.* 42, 1 (1998), 49–69. https://doi.org/10.1002/(SICI)1097-0207(19980515)42:1<49::AID-NME349>3.0.CO;2-2

R. Hauptmann, K. Schweizerhof, and S. Doll. 2000. Extension of the 'solid-shell' concept for application to large elastic and large elastoplastic deformations. *Internat. J. Numer. Methods Engrg.* 49, 9 (2000), 1121–1141. https://doi.org/10.1002/1097-0207(20001130)49:9<1121::AID-NME130>3.0.CO;2-F

Jean Hergel, Kevin Hinz, Sylvain Lefebvre, and Bernhard Thomaszewski. 2019. Extrusion-Based Ceramics Printing with Strictly-Continuous Deposition. *ACM Trans. Graph.* 38, 6, Article 194 (nov 2019), 11 pages. https://doi.org/10.1145/3355089.3356509

T. J. R. Hughes and T. E. Tezduyar. 1981. Finite Elements Based Upon Mindlin Plate Theory With Particular Reference to the Four-Node Bilinear Isoparametric Element. *Journal of Applied Mechanics* 48, 3 (09 1981), 587–596. https://doi.org/10.1115/1.3157679 arXiv:https://asmedigitalcollection.asme.org/appliedmechanics/article-pdf/48/3/587/5879476/587_1.pdf

Geoffrey Irving, Craig Schroeder, and Ronald Fedkiw. 2007. Volume conserving finite element simulations of deformable models. *ACM Transactions on Graphics* 26 (7 2007). Issue 3. https://doi.org/10.1145/1276377.1276394

Ben Jones, Stephen Ward, Ashok Jallepalli, Joseph Perenia, and Adam W. Bargteil. 2014. Deformation embedding for point-based elastoplastic simulation. *ACM Trans. Graph.* 33, 2, Article 21 (apr 2014), 9 pages. https://doi.org/10.1145/2560795

Gergely Klár, Theodore Gast, Andre Pradhana, Chuyuan Fu, Craig Schroeder, Chenfanfu Jiang, and Joseph Teran. 2016. Drucker-prager elastoplasticity for sand animation. *ACM Trans. Graph.* 35, 4, Article 103 (jul 2016), 12 pages. https://doi.org/10.1145/2897824.2925906

Qiqin Le, Yitong Deng, Jiamu Bu, Bo Zhu, and Tao Du. 2023. Second-Order Finite Elements for Deformable Surfaces. In *SIGGRAPH Asia 2023 Conference Papers* (Sydney, Australia) *(SA '23)*. Association for Computing Machinery, New York, NY, USA, Article 113, 10 pages. https://doi.org/10.1145/3610548.3618186

Xuan Li, Minchen Li, and Chenfanfu Jiang. 2022. Energetically consistent inelasticity for optimization time integration. *ACM Trans. Graph.* 41, 4, Article 52 (jul 2022), 16 pages. https://doi.org/10.1145/3528223.3530072

Sebastian Martin, Bernhard Thomaszewski, Eitan Grinspun, and Markus Gross. 2011. Example-based elastic materials. In *ACM SIGGRAPH 2011 Papers* (Vancouver, British Columbia, Canada) *(SIGGRAPH '11)*. Association for Computing Machinery, New York, NY, USA, Article 72, 8 pages. https://doi.org/10.1145/1964921.1964967

E. Miguel, D. Bradley, B. Thomaszewski, B. Bickel, W. Matusik, M. A. Otaduy, and S. Marschner. 2012. Data-Driven Estimation of Cloth Simulation Models. *Comput. Graph. Forum* 31, 2pt2 (may 2012), 519–528.

Juan Montes, Yinwei Du, Ronan Hinchet, Stelian Coros, and Bernhard Thomaszewski. 2023. Differentiable Stripe Patterns for Inverse Design of Structured Surfaces. *ACM Transactions on Graphics (TOG) (to appear)* 42 (2023). Issue 5. https://doi.org/10.1145/3462758

Matthias Müller, Richard Keiser, Andrew Nealen, Mark Pauly, Markus Gross, and Marc Alexa. 2004. Point based animation of elastic, plastic and melting objects. In *Proceedings of the 2004 ACM SIGGRAPH/Eurographics symposium on Computer animation*. 141–151.

Rahul Narain, Tobias Pfaff, and James F. O'Brien. 2013a. Folding and crumpling adaptive sheets. *ACM Transactions on Graphics* 32 (7 2013). Issue 4. https://doi.org/10.1145/2461912.2462010

Rahul Narain, Tobias Pfaff, and James F. O'Brien. 2013b. Folding and crumpling adaptive sheets. *ACM Trans. Graph.* 32, 4, Article 51 (jul 2013), 8 pages. https://doi.org/10.1145/2461912.2462010

Rahul Narain, Armin Samii, and James F. O'Brien. 2012. Adaptive anisotropic remeshing for cloth simulation. *ACM Transactions on Graphics* 31 (11 2012). Issue 6. https://doi.org/10.1145/2366145.2366171

James F. O'Brien. 2002. Graphical modeling and animation of ductile fracture. In *Proceedings of the 29th International Conference on Computer Graphics and Interactive Techniques. Electronic Art and Animation Catalog*. (San Antonio, Texas) *(SIGGRAPH '02)*. Association for Computing Machinery, New York, NY, USA, 161. https://doi.org/10.1145/2931127.2931215

H. Parisch. 1995. A continuum-based shell theory for non-linear applications. *Internat. J. Numer. Methods Engrg.* 38, 11 (1995), 1855–1883. https://doi.org/10.1002/nme.1620381105

Tobias Pfaff, Rahul Narain, Juan Miguel de Joya, and James F. O'Brien. 2014. Adaptive Tearing and Cracking of Thin Sheets. *ACM Transactions on Graphics* 33, 4 (July 2014), xx:1–9. https://doi.org/0.1145/2601097.2601132 To be presented at SIGGRAPH 2014, Vancouver.

Jesús Pérez, Miguel A. Otaduy, and Bernhard Thomaszewski. 2017. Computational design and automated fabrication of Kirchhof-Plateau surfaces. *ACM Transactions on Graphics* 36 (2017). Issue 4. https://doi.org/10.1145/3072959.3073695

Olivier Rémillard and Paul G. Kry. 2013. Embedded thin shells for wrinkle simulation. *ACM Transactions on Graphics* 32 (7 2013). Issue 4. https://doi.org/10.1145/2461912.2462018

C. Sansour. 1995. A theory and finite element formulation of shells at finite deformations involving thickness change: Circumventing the use of a rotation tensor. *Archive of Applied Mechanics* 65, 3 (March 1995), 194–216. https://doi.org/10.1007/bf00799298

J. C. Simo and M. S. Rifai. 1990. A class of mixed assumed strain methods and the method of incompatible modes. *Internat. J. Numer. Methods Engrg.* 29, 8 (1990), 1595–1638. https://doi.org/10.1002/nme.1620290802 arXiv:https://onlinelibrary.wiley.com/doi/pdf/10.1002/nme.1620290802

Demetri Terzopoulos and Kurt Fleischer. 1988. Modeling inelastic deformation: viscoelasticity, plasticity, fracture. *SIGGRAPH Comput. Graph.* 22, 4 (jun 1988), 269–278. https://doi.org/10.1145/378456.378522

Demetri Terzopoulos, John Platt, Alan Barr, and Kurt Fleischer. 1987. Elastically Deformable Models. *SIGGRAPH Comput. Graph.* 21, 4 (aug 1987), 205–214. https://doi.org/10.1145/37402.37427

Bernhard Thomaszewski, Markus Wacker, and Wolfgang Straßer. 2006. A Consistent Bending Model for Cloth Simulation with Corotational Subdivision Finite Elements. In *ACM SIGGRAPH / Eurographics Symposium on Computer Animation*, Marie-Paule Cani and James O'Brien (Eds.). The Eurographics Association. https://doi.org/10.2312/SCA/SCA06/107-116

Pascal Volino and Nadia Magnenat-Thalmann. 2006. Simple Linear Bending Stiffness in Particle Systems. In *ACM SIGGRAPH / Eurographics Symposium on Computer Animation*, Marie-Paule Cani and James O'Brien (Eds.). The Eurographics Association. https://doi.org/10.2312/SCA/SCA06/101-105

Huamin Wang, James F. O'Brien, and Ravi Ramamoorthi. 2011. Data-Driven Elastic Models for Cloth: Modeling and Measurement. *ACM Transactions on Graphics* 30 (7 2011), 1–12. Issue 4. https://doi.org/10.1145/2010324.1964966

Nicholas J. Weidner, Kyle Piddington, David I.W. Levin, and Shinjiro Sueda. 2018. Eulerian-on-lagrangian cloth simulation. *ACM Transactions on Graphics* 37 (2018). Issue 4. https://doi.org/10.1145/3197517.3201281

Jiahao Wen and Jernej Barbič. 2023. Kirchhoff-Love Shells with Arbitrary Hyperelastic Materials. *ACM Trans. Graph.* 42, 6, Article 174 (dec 2023), 15 pages. https://doi.org/10.1145/3618405

Martin Wicke, Daniel Ritchie, Bryan M. Klingner, Sebastian Burke, Jonathan R. Shewchuk, and James F. O'Brien. 2010. Dynamic local remeshing for elastoplastic simulation. In *ACM SIGGRAPH 2010 Papers* (Los Angeles, California) *(SIGGRAPH '10)*. Association for Computing Machinery, New York, NY, USA, Article 49, 11 pages. https://doi.org/10.1145/1833349.1778786

Chris Wojtan, Nils Thürey, Markus Gross, and Greg Turk. 2009. Deforming meshes that split and merge. In *ACM SIGGRAPH 2009 Papers* (New Orleans, Louisiana) *(SIGGRAPH '09)*. Association for Computing Machinery, New York, NY, USA, Article 76, 10 pages. https://doi.org/10.1145/1576246.1531382

O. C. Zienkiewicz, R. L. Taylor, and J. Z. Zhu. 2013. Chapter 13 - Plate Bending Approximation: Thin and Thick Plates. In *The Finite Element Method: its Basis and Fundamentals (Seventh Edition)* (seventh edition ed.), O. C. Zienkiewicz, R. L. Taylor, and J. Z. Zhu (Eds.). Butterworth-Heinemann, Oxford, 407–466. https://doi.org/10.1016/B978-1-85617-633-0.00013-7